

Theoretical and experimental studies of the transverse dielectric properties of KD_2PO_4

S. Havlin, E. Litov, and H. Sompolinsky

Department of Physics, Bar-Ilan University, Ramat-Gan, Israel

(Received 5 January 1976)

The transverse dielectric constant of KD_2PO_4 was measured in the temperature range $79 < T < 322^\circ\text{K}$. A large discontinuity appears at the transition temperature T_c indicating a well-defined first-order transition. A new feature of the data is a dome-shaped figure above T_c , resembling the magnetic susceptibility of many antiferromagnetic materials. Extension of a well-known pseudospin model for KH_2PO_4 to the transverse direction is achieved by taking into account the direct contribution of the displacements of the protons to the transverse polarization. Calculation of the transverse susceptibility for this model within the four-cluster approximation leads to a new independent determination of the Slater-Takagi energy configuration parameters ϵ_0 and ϵ_1 . Excellent fit to the data is achieved for the choices $\epsilon_0/k_B = 92^\circ\text{K}$, $\epsilon_1/k_B = 907^\circ\text{K}$ and indicates that the tunneling integral for KD_2PO_4 is negligible. These values are very close to those derived by independent measurements of ultrasonic sound velocity and specific heat. The results of the model are also compared with the available data for the transverse susceptibility of CsH_2AsO_4 .

I. INTRODUCTION

The dielectric properties of potassium dihydrogen phosphate (KDP)-type crystals in the ferroelectric direction have been extensively studied, both experimentally and theoretically.¹⁻⁴ For the ferroelectric region, these dielectric measurements are uncertain due to the presence of many small ferroelectric domains, and therefore could hardly be used for theoretical interpretation. This is also true for other physical properties such as the spontaneous polarization and ultrasonic sound velocity which can be measured only in the presence of a sizeable biasing electric field.^{5,6} These applied fields however, have the effect of seriously suppressing all critical behavior, resulting in a great loss of valuable information about the phase transition. Information, about the dielectric properties below T_c , which is not affected by domains has been obtained only indirectly through Brillouin-scattering⁶ and heat-capacity⁷ measurements. However, the above difficulties regarding the longitudinal dielectric measurements below T_c do not apply to dielectric measurements in the transverse x direction. In this case, the dielectric constant ϵ_x is not affected by the presence of domains. Evidence for the phase transition is clearly seen in the anomalous behavior of ϵ_x in the temperature range near T_c .^{8,9} Therefore, high-resolution measurements of ϵ_x below T_c will provide direct information on the dielectric properties below T_c . Furthermore, any model proposed for KDP should be capable of simultaneously describing its longitudinal and transverse properties. The interpretation of the transverse dielectric measurements through the proposed model should, therefore, provide direct information about the microscopic parameters which determine the be-

havior of the crystal below as well as above T_c .

Havlin, Litov, and Uehling¹⁰ have recently demonstrated that the pseudospin model of ferroelectricity for KDP-type crystals can be extended to provide a description of the observed transverse susceptibility χ_x . The extended model is based on the contribution of the proton displacements along the x, y bonds to the transverse polarization. It was shown that the temperature dependence of χ_x exhibits antiferroelectric characteristics along the x axis simultaneously with the ferroelectric properties along the z axis. The transverse susceptibility was calculated within the molecular-field approximation (MFA) and its comparison with Busch's data⁸ for KH_2PO_4 taken in 1938 has provided numerical values for two important parameters of the model, the tunneling integral Γ and the effective proton-proton interaction J . The resulting fit to the data was particularly good above T_c but was poor below it. Specifically, the above theory did not account for the observed sharp decrease in the value of χ_x below T_c . This discrepancy is connected to the well-known fact¹ that the MFA does not give a good description of the phase transition, especially below T_c . This is exemplified by the failure of the MFA to account for the sharp rise of the spontaneous polarization with cooling below T_c .

In this paper we report the results of new theoretical and experimental studies of the transverse dielectric properties of KD_2PO_4 . The results of new high-resolution measurements of ϵ_x in KD_2PO_4 as well as a more realistic solution of our extended pseudospin Hamiltonian are presented. The present treatment is limited to the case of zero tunneling integral which is indeed the known situation in KD_2PO_4 .¹¹ The new solution of our model is based on the four-particle approximation

which was previously used successfully to describe the static properties along the z direction.^{1,12,13} The advantage of this approximation over the MFA is that, in addition to the long-range molecular-field two-body forces, the Slater-Takagi³ short-range four-body interactions are also taken into account.

Our new theoretical results vastly improve the fit to the data below T_c and, we suggest, explain the observed sharp anomalous behavior of ϵ_x in this temperature region. Furthermore, our present results, based on the cluster approximation enable us to fix the Slater-Takagi energy parameters in a new, independent way. The resulting value for these parameters turned out to be in very good agreement with those derived from measurements of ultrasonics⁵ and specific heat.⁷

II. EXPERIMENT

Dielectric measurements along the tetragonal x axis at a frequency of 1 kHz were performed in a standard double shield cell. A GR1616 three leads capacitance bridge was used with two PAR model HR8 phase sensitive detectors as a vector lock-in amplifier for the bridge voltage. The bridge accuracy is 10 ppm and its sensitivity 10^{-7} pF. A high-quality x -cut KD_2PO_4 crystal, with 98% deuteration level was bought from Cleveland Crystals, Inc. The dimensions of the crystal were $1 \times 12 \times 12$ mm³ and its x faces were evaporated with chrome and gold. The orientation deviation of the x axis from the crystals' true axis was reported to be within 0.25 of a degree. It can be easily shown, that the error due to the interference of the z component of the dielectric constant caused by this amount of deviation is negligible. Temperature stability of ± 0.5 mK was easily achieved using home made temperature controls and temperature baths of acetone mixed with dry ice for the region above 200°K and liquid N_2 for the region below it.

The temperature was measured using a platinum-resistor thermometer supplied and calibrated by the Rosemount Engineering Co. (model MA 200 D). A four-leads technique was employed in the measurements of the thermometer resistance using a Leeds and Northrop K-5 potentiometer, in order to eliminate leads resistance. The absolute precision of the temperature was $\pm 0.04^\circ\text{K}$. The dielectric constant was measured point by point to ensure thermal equilibrium in the sample. The total uncertainty in ϵ_x is estimated to be less than 1%.

III. EXPERIMENTAL RESULTS

The temperature dependence of the dielectric constant ϵ_x of KD_2PO_4 from 120°K to above room

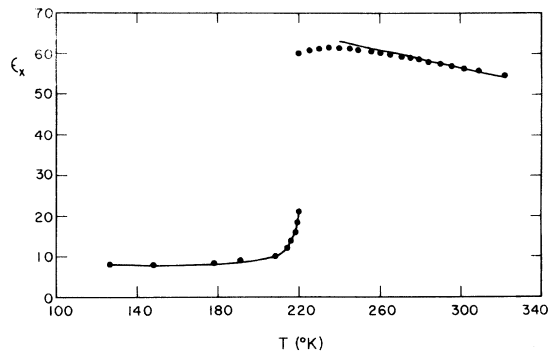


FIG. 1. Transverse dielectric constant ϵ_x of KD_2PO_4 vs temperature. The points are the experimental data. The line is the theoretical result based on Eq. (14). The best fit to the experimental results was achieved with the Slater-Takagi energy parameters and the transverse dipole moment given in Table III.

temperature is shown Fig. 1, and the numerical values for the entire temperature range are listed in Table I. It is seen that below T_c , ϵ_x has a very strong anomalous temperature behavior, rising from a value of $\epsilon_x = 7.73$ at 80°K to $\epsilon_x = 22.8$ just below T_c . The sharp discontinuity at T_c is vividly seen in Fig. 2, giving evidence that the transition is of first order as was confirmed in the ultrasonic¹⁵ and specific-heat⁷ measurements. Above T_c an interesting new feature appearing in the data is a dome-shaped figure, strongly resembling the temperature dependence of susceptibility of several antiferromagnets above T_c .¹⁴ An extended view of that portion of the curve is shown in Fig. 3. The peak of ϵ_x does not coincide with the transition temperature $T_c = 220.42^\circ\text{K}$, but falls 15°K above T_c at $T = 235.2^\circ\text{K}$.

IV. THEORY

In order to incorporate the transverse dipole moments of the hydrogen bonds we use the following extended pseudospin Hamiltonian:

$$\begin{aligned} \mathcal{H} = & -\Gamma \sum_i S_i^z - \frac{1}{2} \sum_{i,j} J_{ij} S_i^z S_j^z \\ & - \mu_x E_x \left(\sum_i^+ S_i^z - \sum_i^- S_i^z \right) \\ & - \mu_y E_y \left(\sum_i^+ S_i^z - \sum_i^- S_i^z \right). \end{aligned} \quad (1)$$

The first term represents the tunneling motion of the proton in the hydrogen bond. The second term represents the effective proton-proton interaction, in which, as will be shown later, J_{ij} are related to the Slater-Takagi energy levels ϵ_0 and ϵ_1 . The quantity S_i is the usual Ising operator whose z component S_i^z represents the two possible equilibrium positions of the i th proton in its bond. The

TABLE I. Transverse dielectric constant data for KD_2PO_4 .

T (K)	ϵ_x	T (K)	ϵ_x
78.9	7.73	234.218	61.3562
113.73	7.83	234.552	61.3577
126.82	7.89	234.878	61.3577
148.63	8.01	235.191	61.3578
178.03	8.29	235.516	61.3572
196.33	8.93	235.857	61.3557
207.89	10.26	236.187	61.354
213.82	12.33	236.495	61.351
215.00	13.02	236.977	61.347
216.029	13.801	237.402	61.341
217.058	14.834	237.857	61.334
217.927	15.982	238.297	61.327
218.626	17.235	238.574	61.322
219.128	18.429	239.005	61.312
219.482	19.506	239.427	61.302
219.736	20.482	239.743	61.295
219.912	21.348	240.318	61.279
220.086	22.315	240.786	61.265
220.145	22.840	242.839	61.182
220.424	59.982	244.728	61.105
220.464	59.995	247.35	60.97
221.164	60.164	249.37	60.86
221.873	60.322	251.87	60.71
222.678	60.481	253.52	60.61
223.652	60.648	256.68	60.39
224.122	60.771	260.50	60.10
225.401	60.878	265.43	59.71
226.492	60.999	270.68	59.27
227.716	61.097	276.11	58.80
228.665	61.164	279.24	58.52
229.452	61.226	284.11	58.09
230.666	61.281	290.06	57.56
231.570	61.320	295.98	57.04
232.951	61.342	309.33	55.85
233.801	61.353	321.66	54.85

last two terms represent the interaction of the external transverse fields E_x and E_y with the transverse dipole moments μ_x and μ_y associated with the protonic displacements along their bonds.¹⁰ The symbol $\sum_{x,y}^{\pm}$ means summation over plus and minus bonds, aligned along the x and y directions. A bond is labeled plus (minus) when the displacements of its proton towards its spin-up position contributes positively (negatively) to the polarization along x or y directions as described in Fig. 4.

Since the x and y directions in KDP are equivalent above T_c and only slightly different below T_c we assume that the transverse susceptibility is isotropic in the x - y plane, and the field direction can be chosen at will. For convenience we choose it along the 45° direction, resulting in a simpler form for the field term

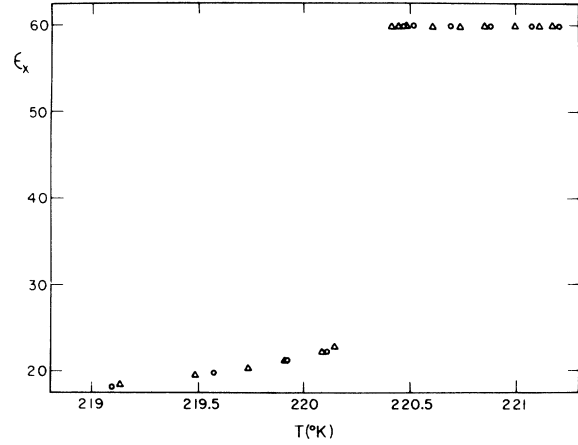


FIG. 2. Experimental data of ϵ_x near the transition temperature is given on a greatly expanded temperature scale. The triangular points are the data obtained on cooling whereas the circular points are the data obtained on heating.

$$-\mu_x E_x \left(\sum_i^+ S_i^z - \sum_i^- S_i^z \right),$$

where now \sum^{\pm} means that the sum is to be taken over plus and minus x and y bonds. A more detailed explanation of the field term is given in Ref. 10.

The Hamiltonian with this form for the field and without tunneling is similar to that of an Ising antiferromagnet Hamiltonian. Numerical results for the susceptibility were given by Fisher and Sykes¹⁴ in terms of an isotropic nearest-neighbor interaction parameter J . In KDP however, the interaction between neighbors is anisotropic¹³ and the above mentioned results are not directly applicable. As a first attempt to incorporate anisotropic interaction into the antiferromagnet Ising model, we apply the four-cluster approximation to our model. In this approximation we take into account the four-cluster short-range forces to-

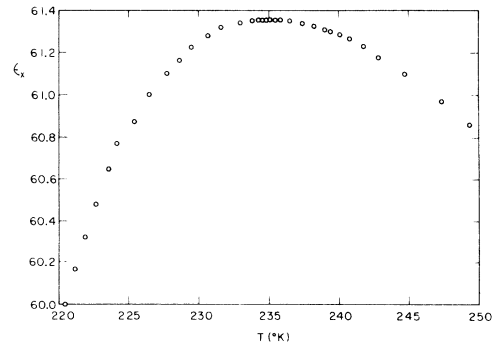


FIG. 3. Experimental data of ϵ_x in the dome-shaped region between 220 and 250 °K.

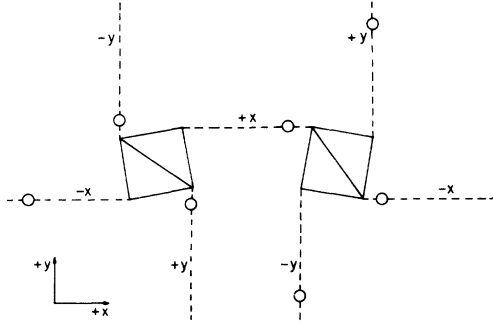


FIG. 4. Z-axis projection of the hydrogen bonds connecting the K-PO₄ groups showing the different labels of the six nearest neighbors of a plus-x bond.

gether with molecular-field long-range interaction. Since there is enough evidence that the tunneling integral is negligible in KD₂PO₄,¹¹ we will not include it at this stage.

The four-particle Hamiltonian in the cluster approximation, with a field in the *x*-*y* plane pointing along the 45° direction, can be shown to be of the form

$$H_4 = -V(S_1^x S_2^x + S_2^x S_3^x + S_3^x S_4^x + S_4^x S_1^x) - U(S_1^x S_3^x + S_2^x S_4^x) - (\gamma \langle S^z \rangle + \frac{1}{2} \Delta_x)(S_1^x + S_2^x + S_3^x + S_4^x) - (\mu_x E_x + \frac{1}{2} \Delta_x)(S_1^x + S_2^x - S_3^x - S_4^x), \quad (2)$$

where *U* and *V* are related to the Slater-Takagi parameters by

$$4U = -2\epsilon_1 + 2\epsilon_0; \quad 4V = 2\epsilon_1 - \epsilon_0. \quad (3)$$

Here γ represents the long-range interaction energy, Δ_x and Δ_z are the effective-field energies along the *x* and *z* directions, respectively, produced by the adjacent bonds outside the cluster. Below *T_c*, Δ_z does not vanish even when the transverse field is removed due to the appearance of the spontaneous polarization. However, $\Delta_x = 0$ when $E_x = 0$ above and below *T_c*. The quantity $\langle S^z \rangle$ is the normalized polarization along the *z* direction and is given by

$$\langle S^z \rangle = \frac{1}{2}(\langle S_+^z \rangle + \langle S_-^z \rangle), \quad (4)$$

where $\langle S_{\pm}^z \rangle$ is the normalized average polarization of a \pm bond. $\langle S^z \rangle$ is related to the total polarization along the *z* direction by $P_z = 2N\mu_x \langle S^z \rangle$, where *N* is the number of PO₄ groups per unit volume and μ_x is the longitudinal dipole moment associated with one hydrogen bond.

The one-particle Hamiltonian for the plus and minus bonds is given by

$$H_+ = -(\gamma \langle S^z \rangle + \Delta_x + \Delta_z + \mu_x E_x) S_{1,2}^x, \quad (5)$$

$$H_- = -(\gamma \langle S^z \rangle + \Delta_x - \Delta_z - \mu_x E_x) S_{3,4}^x.$$

In order to calculate the order parameters $\langle S_+^z \rangle$ and $\langle S_-^z \rangle$ of the plus and minus bonds it is necessary, first, to eliminate Δ_x and Δ_z with the aid of the cluster equilibrium conditions

$$\frac{\partial F}{\partial \Delta_x} = \frac{\partial F}{\partial \Delta_z} = 0. \quad (6)$$

Here *F* is the Helmholtz free energy and is given by

$$F = -k_B T (\ln Z_+ - \ln Z_- - \ln Z_0) + \gamma \langle S^z \rangle^2, \quad (7)$$

where *Z_±* and *Z₀* are the partition functions of the one and four-particle Hamiltonians *H_±* and *H₀*, respectively. From Eqs. (6) and (7) it follows that the order parameter $\langle S_+^z \rangle$ and $\langle S_-^z \rangle$ are given by

$$\langle S_+^z \rangle = \frac{\text{Tr}[S_{1,2}^z \exp(-\beta H_+)]}{\text{Tr} \exp(-\beta H_+)} = \frac{\text{Tr}[S_{1,2}^z \exp(-\beta H^+)]}{\text{Tr} \exp(-\beta H^+)},$$

$$\langle S_-^z \rangle = \frac{\text{Tr}[S_{3,4}^z \exp(-\beta H_-)]}{\text{Tr} \exp(-\beta H_-)} = \frac{\text{Tr}[S_{3,4}^z \exp(-\beta H^-)]}{\text{Tr} \exp(-\beta H^-)}, \quad (8)$$

where $\beta = 1/k_B T$.

The energy levels, of the four-particle Hamiltonian *H₄* in the presence of the external transverse field, required for the solution of Eqs. (8) are easily calculated from Eq. (2), and the results are summarized in Table II. The corresponding energy levels in the Slater-Takagi models are also included in the table. It should be pointed out that the transverse field splits the energy levels differently from a field directed along the *z* axis.¹³

After substituting the values for the energy levels in Eq. (8), and after some algebra, one obtains the following relations for $\langle S_+^z \rangle$ and $\langle S_-^z \rangle$:

$$\langle S_+^z \rangle = \langle S^z \rangle + (1 - \langle S^z \rangle^2)(1 + \alpha)\beta\mu_x E_x, \quad (9)$$

$$\langle S_-^z \rangle = \langle S^z \rangle - (1 - \langle S^z \rangle^2)(1 + \alpha)\beta\mu_x E_x.$$

The quantity α is defined as

$$\alpha = \frac{2 \cosh^2 x (A + L \cosh x)}{K - 1 + 4L \cosh x - 2(A - 1) \cosh^2 x - 2L \cosh^3 x} - 1, \quad (10)$$

where

$$A = \exp(-\beta\epsilon_0), \quad L = \exp(-\beta\epsilon_1),$$

$$K = 2A + \exp\beta(2\epsilon_0 - 4\epsilon_1),$$

and

$$x = \tanh^{-1} \langle S^z \rangle + \beta\gamma \langle S^z \rangle.$$

As follows from Eq. (8), the average polarization in the *z*-direction $\langle S^z \rangle$ which appears in Eq. (9) satisfies the following consistency relation:

$$\langle S^z \rangle = \frac{2L \sinh x + \sinh 2x}{4L \cosh x + \cosh 2x + K}. \quad (11)$$

TABLE II. Energy levels of the four-cluster Hamiltonian H_4 , Eq. (2), for the various proton configurations.

$S_1^z S_2^z S_3^z S_4^z$	No. of adjacent protons	Eigenvalues of H_4	Slater-Takagi energy levels			
+	+	+	+	2	$-2(U+2V) - 4(\frac{1}{2}\Delta_z + \gamma \langle z \rangle)$	$-4(\frac{1}{2}\Delta_z + \gamma \langle z \rangle)$
-	-	-	-	2	$-2(U+2V) + 4(\frac{1}{2}\Delta_z + \gamma \langle z \rangle)$	$+4(\frac{1}{2}\Delta_z + \gamma \langle z \rangle)$
+	+	-	-	2	$2U - 4(\mu_x E_x + \frac{1}{2}\Delta_x)$	$\epsilon_0 - 4(\mu_x E_x + \frac{1}{2}\Delta_x)$
-	-	+	+	2	$2U + 4(\mu_x E_x + \frac{1}{2}\Delta_x)$	$\epsilon_0 + 4(\mu_x E_x + \frac{1}{2}\Delta_x)$
-	+	+	-	2	$2U$	ϵ_0
+	-	-	+			
+	+	-	+	1	$-2[\mu_x E_x + \frac{1}{2}(\Delta_z + \Delta_x) + \gamma \langle z \rangle]$	$\epsilon_1 - 2[\mu_x E_x + \frac{1}{2}(\Delta_z + \Delta_x) + \gamma \langle z \rangle]$
+	+	+	-	3		
-	-	+	-	3	$2[\mu_x E_x + \frac{1}{2}(\Delta_z + \Delta_x) + \gamma \langle z \rangle]$	$\epsilon_1 + 2[\mu_x E_x + \frac{1}{2}(\Delta_z + \Delta_x) + \gamma \langle z \rangle]$
-	-	-	+	1		
-	+	+	+	1	$-2[-\mu_x E_x + \frac{1}{2}(\Delta_z - \Delta_x) + \gamma \langle z \rangle]$	$\epsilon_1 - 2[-\mu_x E_x + \frac{1}{2}(\Delta_z - \Delta_x) + \gamma \langle z \rangle]$
+	-	+	+	3		
+	-	-	-	3	$2[-\mu_x E_x + \frac{1}{2}(\Delta_z - \Delta_x) + \gamma \langle z \rangle]$	$\epsilon_1 + 2[-\mu_x E_x + \frac{1}{2}(\Delta_z - \Delta_x) + \gamma \langle z \rangle]$
-	+	-	-	1		
-	+	-	+	0	$-2(U-2V)$	$4\epsilon_1 - 2\epsilon_0$
+	-	+	-	4		

Since $\langle S^z \rangle$ is not affected by the transverse field, Eq. (11) is the same as the consistency relation for the spontaneous polarization in the free-field case as previously derived in Refs. 1 and 3. Solution of Eq. (11) gives a first- or a second-order transition depending on the choice of the energy parameters ϵ_0 , ϵ_1 , and the long-range order parameter γ . For a more detailed discussion see the Appendix.

From the above discussion about the transverse-field term in the Hamiltonian, Eq. (1), it follows readily that the average transverse polarization is given by

$$P_x = \frac{1}{2} N \mu_x (\langle S_x^+ \rangle - \langle S_x^- \rangle). \quad (12)$$

The transverse susceptibility χ_x ,

$$\chi_x = \left. \frac{dP_x}{dE_x} \right|_{E_x=0}, \quad (13)$$

is calculated from Eq. (9) and is found to be

$$\chi_x = (N \mu_x^2 / k_B T) (1 + \alpha) (1 - \langle S^z \rangle^2). \quad (14)$$

It is seen that the transverse susceptibility χ_x strongly depends on the spontaneous polarization along the z direction. A plot of Eq. (10) shows that the parameter α appearing in Eq. (14) has a relative weak temperature dependence for $T < T_c$, even in the phase transition region, see Fig. 5. Hence the dominant term of χ_x below T_c is $1 - \langle S^z \rangle^2$. For

a first-order transition there will be a discontinuity in the spontaneous polarization P_z at T_c , resulting also, through Eq. (14), in a discontinuity in χ_x .

For $T > T_c$, $\langle S^z \rangle = 0$ and χ_x is reduced to

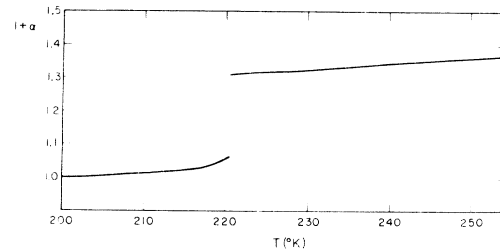
$$\chi_x = \frac{2N \mu_x^2}{k_B T} \left(\frac{\exp(-\beta \epsilon_0) + \exp(-\beta \epsilon_1)}{1 + 2 \exp(-\beta \epsilon_1) + \exp(\beta(2\epsilon_0 - 4\epsilon_1))} \right). \quad (15)$$

It will be noticed that the long-range interaction parameter γ does not appear in χ_x above T_c , due to the fact that the term $\gamma \langle S^z \rangle$ in the Hamiltonian vanishes above T_c for $E_z = 0$.

An expansion of Eq. (15) for $T > T_c$ gives

$$\chi_x \approx C / (T + \Theta), \quad (16)$$

where for $\beta \epsilon_1 \gg 1$

FIG. 5. Plot of $1 + \alpha$, Eq. (10), vs temperature.

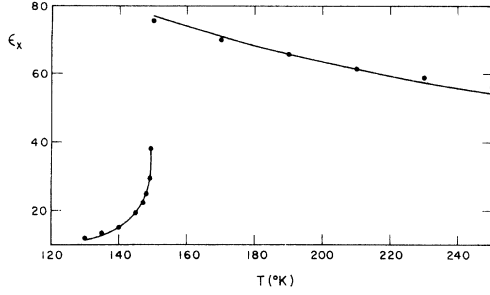


FIG. 6. Temperature dependence of the transverse dielectric constant ϵ_x of CsH_2AsO_4 . The dots are the experimental data measured by R. J. Pollina and C. W. Garland (Ref. 15). Best fit was achieved with the Slater-Takagi energy parameters and the transverse dipole-moment given in Table III.

$$C \simeq (2N\mu_x^2/k_B)e^{-y}/(1-y); \quad y \equiv \beta_c \epsilon_0$$

and

$$\Theta \simeq T_c[y/(1-y)].$$

is a positive number. Thus, the transverse susceptibility in KDP is antiferroelectric in character, as is expected from the known crystal structure and as is indicated by the present experiments where $\Theta > 0$.

V. COMPARISON OF THEORY WITH EXPERIMENT

In this section we will compare the theory presented in Sec. IV with the experimental data for the transverse dielectric constant ϵ_x for KD_2PO_4 , measured in our laboratory, as well as with the data for CsH_2AsO_4 (CDA), measured by Pollina and Garland.¹⁵ It is known that the tunneling integral Γ for KD_2PO_4 is very small,^{1,2,11} a fact that is consistent with our neglecting Γ in the model. However, there is some uncertainty regarding the value of Γ for CsH_2AsO_4 ,^{2,11} and this will be discussed later in the context of the present model.

Consulting the data for ϵ_x (see Figs. 1 and 2) it will be noted that there is a discontinuity in ϵ_x at the transition temperature T_c . As stated above this is due to the discontinuity in the spontaneous polarization P_z , indicating a first-order transition. In order to apply the theory to a first order

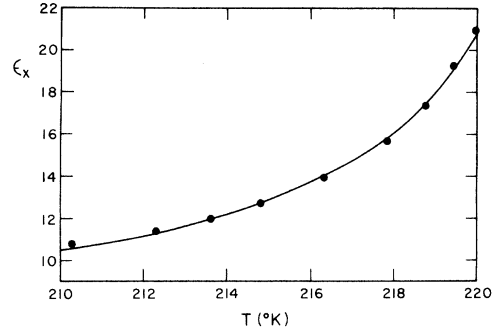


FIG. 7. Comparison between the theoretical and experimental results of ϵ_x in KD_2PO_4 for the transition region below T_c .

case we have taken into account the appropriate conditions which lead to a relation among ϵ_0 , ϵ_1 , γ , and T_c . These aspects are discussed in the Appendix.

Comparison of $\epsilon_x = 4\pi\chi_x + 1$, Eq. (14), with the experimental data for KD_2PO_4 and CsH_2AsO_4 in the whole temperature range is shown in Fig. 1 and Fig. 6, respectively. We present, also in Fig. 7 the comparison between theory and experiment for the range immediately below T_c , in KD_2PO_4 . The sets of parameters which give the best fit with experiment and which also satisfy Eq. (A5) of the Appendix are given in Table III. It should be emphasized that only one set of parameters has been used for the entire temperature range (above and below T_c). Background susceptibilities of $6.7/4\pi$ for KD_2PO_4 and $10/4\pi$ for CsH_2AsO_4 , which is clearly indicated in the experiments were taken into account in the evaluation of the data.

As can be seen from Figs. 1 and 7 the fit of ϵ_x for KD_2PO_4 is excellent for the entire transition temperature range except for the dome-shape region. Since the dome-shaped dependence of ϵ_x on temperature is not predicted by the present treatment of our model, we have excluded that part of the data from the fitting procedure. However, it is noticed that our Hamiltonian, Eq. (1) is similar in form to that of an Ising antiferromagnet Hamiltonian and its solution by the series expansion method predicts this shape quite ade-

TABLE III. Parameters which give the best fit between the present theory and experimental data for the transverse dielectric constant ϵ_x .

Crystal	T_c (°K)	P_c	ϵ_0/k_B (°K)	ϵ_1/k_B (°K)	γ/k_B (°K)	$10^{18}\mu_x$ (cgs)
KD_2PO_4 (dKDP)	220.426	0.826	92	907	37.1	3.3
CsH_2AsO_4 (CDA)	149.75	0.71	55	495	32.6	2.9

TABLE IV. Comparison of the Slater-Takagi configuration energies and the long-range interaction γ derived from the present measurements of ϵ_x for KD_2PO_4 with those derived from ultrasonic and specific-heat measurements.

Experiment	ϵ_0/k_B (°K)	ϵ_1/k_B (°K)	γ/k_B (°K)
Transverse dielectric constant	92	907	37.1
Ultrasonics	92.3	900	30.0
Specific heat	94.3	900	35.6

quately.¹⁴ Except for the dome-shaped region, the maximum deviation between theory and experiment is 4%, however, above 200°K the deviation is less than 2%. It should be mentioned that for the undeuterated crystal KH_2PO_4 we were not able to explain the whole transition range (above and below T_c) with a single set of parameters, and with $\Gamma=0$.⁹ This indicates that the tunneling integral is negligible for KD_2PO_4 but significant in KH_2PO_4 , a fact which was recognized previously.^{1,13}

Since the parameters presented in Table III describe adequately the transverse susceptibility χ_x , they should according to the model also describe other physical properties associated with this ferroelectric transition. Indeed the parameters given in Table III are very close to those derived from ultrasonics¹⁶ and specific-heat⁷ measurements (see Table IV). The smaller value of γ derived from ultrasonics is due to the fact that because of different amount of deuteration the crystal in the ultrasonic measurements had a lower transition temperature $T_c=205.6^\circ\text{K}$, compared to $T_c \cong 220^\circ\text{K}$ in the other experiments. In addition one of the basic properties of the transition is the spontaneous polarization P_s . Thus in order to test our independently derived set of parameters, we have calculated P_s using these parameters and compared it with experimental values of P_s which we derived from specific heat measurements by the well-known relation $\langle P_s \rangle^2 \propto \Delta S(T)$, where $\Delta S(T)$ is the temperature-dependent transition entropy.^{11,17} For KD_2PO_4 this comparison is shown in Fig. 8, and as can be seen the fit of the theory to experiment is very good. However, the value of the normalized spontaneous polarization at T_c , $p_c=0.84$, derived in the present work is higher than the value $P_c=0.78$ derived from specific-heat measurements.¹⁸ Similarly it is well known from calorimetric measurements^{7,17} that a set of parameters which describes the properties of the crystal in the whole temperature range predicts a sharper discontinuity at T_c than actually observed. This slight discrepancy between theory and ex-

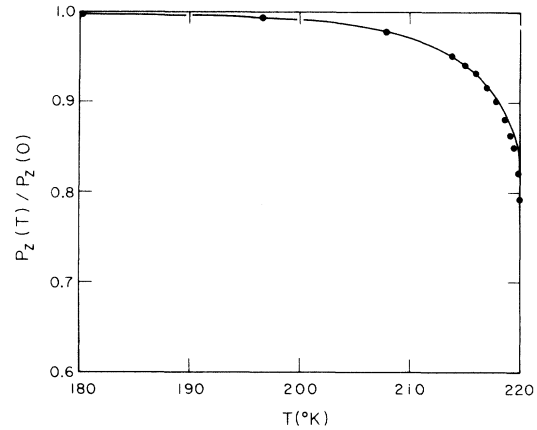


FIG. 8. Temperature dependence of the normalized spontaneous polarization of KD_2PO_4 . The points are derived from specific-heat measurement done by W. Reese and L. F. May (Ref. 7). The line represents the theoretical calculation based on Eq. (11) and on the Slater-Takagi energy parameters which give the best fit for the data of ϵ_x (Table III).

periment at T_c is attributed to the usual failure of the mean-field theory to account for the phenomena in the immediate vicinity of the phase transition.⁷

For CsH_2AsO_4 the theory describes quite well the data for ϵ_x (see Fig. 6), however there is small deviation between theory and experiment. It should also be noted that the values of the configurational energy parameters of CDA which are given in Table III are smaller than those reported for specific heat measurements.^{2,17} These discrepancies are possibly due to the neglect of the tunneling in the present theory, thus indicating the existence of tunneling in CDA.²

It should be noted that the values of the transverse dipole moments μ_x which were derived in the present treatment (Table III) are smaller than the values derived in the treatment of our model within the MFA.¹⁰ Thus, the present values of μ_x are closer to the expected dipole-moment of the proton displacements along their bonds.¹⁰ However, these values are still higher than the expected protonic contribution, indicating that other transverse-ion displacements are coupled to the displacements of the protons along the hydrogen bonds.

Finally, it should be noted that whereas for KD_2PO_4 the tunneling term in the Hamiltonian can be neglected it is significant in undeuterated KDP type crystals. A solution of our model which includes tunneling is currently in preparation, for the purpose of explaining the transverse dielectric properties of those KDP type crystals in which the tunneling is significant.

ACKNOWLEDGMENTS

The authors wish to thank Professor M. Luban for critically reading the manuscript, J. Namir for assistance in obtaining the data, and A. Ratzhab and M. Landau for helping with the computer calculations.

APPENDIX

In this Appendix we derive the relationship between the configurational energies ϵ_0 , ϵ_1 and the long-range parameter γ and T_c , for the general case of a first- and second-order transition.

This can be done by solving simultaneously the following two equations:

$$\left. \frac{\partial F}{\partial P_s} \right|_{T_c} = 0, \quad (A1)$$

$$F(p_c) = F(0), \quad (A2)$$

where F is the free energy given in Eq. (7). Note that Eq. (A1) is the usual condition for equilibrium, and Eq. (A2) represents the condition for the transition temperature T_c .

From Eq. (A1) one obtains

$$\gamma = (k_B T_c / p_c) (x - \tanh^{-1} p_c), \quad (A3)$$

and from (A2)

$$\gamma = \frac{k_B T_c}{p_c^2} \ln \frac{Z_4(1-p_c^2)}{2(4L+K+1)}, \quad (A4)$$

where $Z_4 = (2K + \cosh 2x + 4L \cosh x)$. The quantities K , L , A , and x in Eq. (A3) and Eq. (A4) which were defined in Sec. IV are evaluated at T_c .

Eliminating γ from Eqs. (A3) and (A4) one obtains

$$\ln \frac{2(4L+K+1)}{Z_4(1-p_c^2)} + p_c(x - \tanh^{-1} p_c) = 0. \quad (A5)$$

Another relation between x at T_c and p_c is given in Eq. (11). Thus we have two closed equations which determine p_c for a given set of values for ϵ_0 , ϵ_1 , and T_c . For the first-order transitions when $p_c \neq 0$, γ is determined through Eq. (A3). For the second order case, when $p_c = 0$, Eqs. (A1) and (A2) do not yield any relation between T_c and the energy parameters ϵ_0 , ϵ_1 , and γ . However in this case one may use the condition $\partial^2 F / \partial P_s^2 = 0$ which leads³ to

$$\gamma / k_B T_c = (L + \frac{1}{2}K - \frac{1}{2}) / (L + 1). \quad (A6)$$

From this equation one can determine γ for a given set of ϵ_0 , ϵ_1 , and T_c .

¹R. Blinc and S. Svetina, Phys. Rev. **147**, 430 (1966).

²V. G. Vaks, N. E. Zein, and B. A. Strukov, Phys.

Status Solidi A **30**, 801 (1975).

³H. B. Silsbee, E. A. Uehling, and V. H. Schmidt, Phys. Rev. **133**, A165 (1964); J. C. Slater, J. Chem. Phys. **9**, 16 (1941).

⁴G. A. Samara, Ferroelectrics **5**, 25 (1973); R. M. Hill and S. K. Ischiki, Phys. Rev. **130**, 150 (1963); **132**, 1603 (1963); R. Blinc, M. Burgar, and A. Levstik, Solid State Commun. **12**, 573 (1973).

⁵J. W. Benepe and W. Reese, Phys. Rev. B **3**, 3032 (1971); E. Litov and C. W. Garland, *ibid.* **2**, 4597 (1970).

⁶E. M. Brody and H. Z. Cummins, Phys. Rev. B **9**, 179 (1974).

⁷W. Reese and I. F. May, Phys. Rev. **162**, 510 (1967); **167**, 504 (1968); W. Reese, Phys. Rev. **181**, 905 (1969).

⁸G. Busch, Helv. Phys. Acta **11**, 269 (1938).

⁹S. Havlin, E. Litov, and H. Sompolsky, Phys. Lett. **A51**, 33 (1975).

¹⁰S. Havlin, E. Litov, and E. A. Uehling, Phys. Rev. B **9**, 1024 (1974).

¹¹C. W. Fairall and W. Reese, Phys. Rev. B **11**, 2066 (1975).

¹²V. G. Vaks and V. I. Zinenko, Zh. Eksp. Teor. Fiz. **64**, 650 (1973) [Sov. Phys.-JETP **37**, 330 (1973)].

¹³M. Tokunga and T. Matsubara, Prog. Theor. Phys. **35**, 581 (1966).

¹⁴M. E. Fisher and M. F. Sykes, Physica (Utr.) **28**, 939 (1962).

¹⁵R. J. Pollina and C. W. Garland, Phys. Rev. B **12**, 362 (1975).

¹⁶E. Litov and E. A. Uehling, Phys. Rev. B **1**, 3713 (1970).

¹⁷M. Deutsch and E. Litov, Ferroelectrics **7**, 209, (1974).

¹⁸The value $p_c = 0.78$ is slightly different from that derived in Ref. 11, $p_c = 0.724$. This is due to slightly different choice of the background in the specific-heat data.